Rank-reduction de-blending for record length extension - the example of the Carnarvon basin

Margherita Maraschini, Audrey Kielius, Sergio Grion, Dolphin Geophysical.*

Summary

During the summer of 2015 Dolphin Geophysical, in collaboration with project partner TGS, completed the acquisition of the NCB-15 MC3D survey on the Exmouth Plateau, in the Carnarvon basin offshore Western Australia. In order to provide good imaging throughout the thick Triassic section and down to the deep Permian marker, which is at 9.0 - 9.5s in some areas, the survey was designed and acquired using broadband methodologies and long 12s records. Due to shot-point interval and vessel speed constraints the acquisition was performed using an overlapping shot strategy, with the individual shots later recovered via de-blending at the data processing stage. The goal of this paper is to illustrate the de-blending methodology used to remove the shot overlap and the advantages of record length extension.

Introduction

In recent years, continuous recording has become increasingly popular for marine acquisition. Trace length is no longer an acquisition parameter but a processing choice: the dataset is recorded without interruption and is arranged into shot records after the acquisition. Therefore, when information on deep layers is required the processing trace length can be chosen to be longer than the time gap between adjacent shots.

This acquisition and processing strategy has been implemented for the Carnarvon basin survey, where the desired trace length is 12s and the average time gap between adjacent shots is about 8s. In this scenario the overlap of the following shot will hide the deep part of the shot record; in other words in the deep part of the shot record the two sources are blended, and require de-blending during processing.

Several de-blending techniques have been developed over the past few years (Berkhout 2008, Mahdad et al. 2011, Maraschini et al. 2012, Wason et al. 2014, Cheng and Sacchi 2015, Kumar et al. 2015), but most of them are customized to separate almost simultaneous sources, aiming for signal preservation. In this paper we focus on the case where the blending noise amplitude is orders of magnitude higher than the signal, aiming to retrieve as much signal as possible whilst removing all of the blending noise. More details on the methodology and examples of its effectiveness can be found in Maraschini et al. (2016).

Method

The main steps of the processing sequence for the Carnarvon dataset are:

- Data reformat
- Estimation of a shot by shot, far field source signature derived from near field hydrophones and shot by shot source de-signature using a vertical operator
- Swell & cable noise attenuation
- Overlap removal (De-blending)
- Linear noise attenuation in shot domain and SI removal
- De-ghosting
- 3D SRME
- High-resolution Radon demultiple

This paper focuses on the de-blending step. Due to the amplitude decay of the signal with time, the amplitude of the overlapping signal (i.e. the blending noise) can be several orders of magnitude higher than the underlying signal (Figure 3 shows an example of shot records before de-blending). The time gap between source firing times is not constant because of the variability of the vessel velocity, and hence the blending noise appears incoherent in the common channel domain. In the de-blending process we exploit this incoherency to separate signal from blending noise.

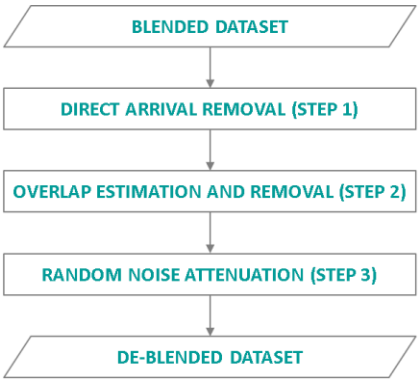

Figure 1: Scheme of the de-blending method.

The de-blending scheme is described in Figure 1:
Step 1: in common shot domain the direct arrival of the overlapping shot is removed by a local *f-k* filter. Additionally, a parabolic radon filter is applied to remove events that are too slow to be signal.

Step 2: the overlapping signal is estimated and removed from the dataset. First, the time delays between firing times are removed: the blending noise will then appear coherent in the common channel domain, while the signal will appear random. Using a rank-reduction filter with a low rank (Maraschini et al. 2012, Cheng and Sacchi 2015 and Kumar et al. 2015) we remove from the dataset all the incoherent energy (which includes the signal, because of the removed time delays) and obtain an estimate of the blending noise. This estimate can then be removed from the dataset.
Step 3: after adding back the time delays, in order to make the signal coherent and the residual blending noise random, a robust rank-reduction filter (Trickett 2003 and Trickett et al. 2012), which is more effective on outliers, is applied in the overlap area. This step allows the residual blending noise to be removed.

Case history

Dolphin Geophysical, in collaboration with project partner TGS, acquired a 3D survey on the Exmouth Plateau, offshore Western Australia (Figure 2). This survey provides ca 13,415 km2 of new 3D coverage over this frontier area. In order to provide good imaging throughout the thick Triassic section and down to the deep Permian marker, which is at 9.0 - 9.5s in some areas, the survey was designed and acquired using broadband methodologies and long 12s records. To achieve this deep imaging objective while maintaining the shot-point interval at 18.75m and vessel speed at 4knots, the acquisition was performed using a shot-overlap strategy with the individual shots then recovered via de-blending.

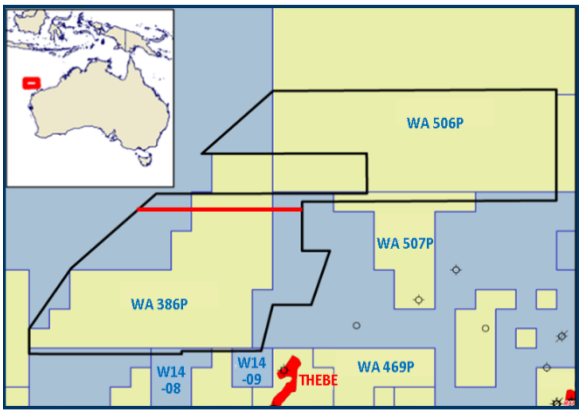

Figure 2: Survey map. The red line represent the sequence used fot the case history.

To define the parameters used in the processing, we performed a synthetic test (Maraschini et al., 2016). We considered an unblended line acquired at a nearby location with visible energy below 10s, and we synthetically blended it with itself, using the real time delays of an adjacent line. Then we run a parametric analysis on the filtering parameters, in order to optimize a processing sequence able to retrieve the hidden energy. Finally, we applied this processing sequence to the real data

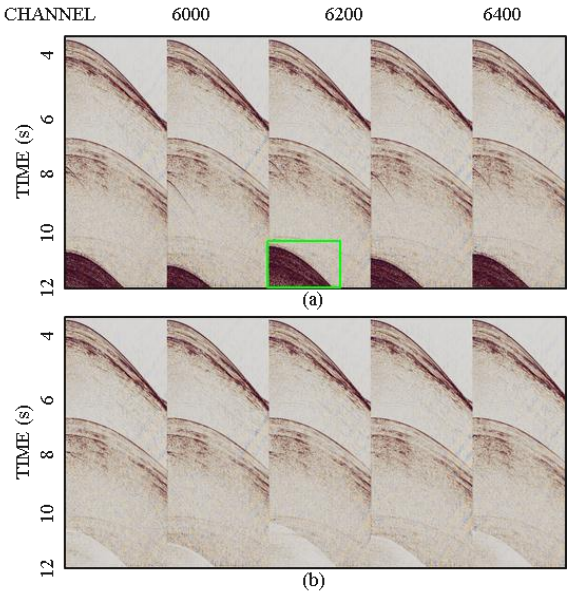

Figure 3: Example of shot records. The green rectangle indentificates the area zoomed in Figure 4. a) before de-blending; b) after de-blending

The red line in Figure 2 represents the CMP line used in the following figures. Figure 3 shows five adjacent shot records before and after de-blending. We note that the time gap between source firing times is not constant (i.e. the overlapping signals appear at variable times): this feature of the dataset will be exploited in the de-blending code. Figure 4 illustrates each step of the de-blending procedure for the area in the green rectangle in Figure 3a. In the first step (Figure 4b) several noise attenuation tools are applied in the common shot domain: an f-k dip filter is applied to remove the direct arrival (not shown) and a parabolic radon filter is applied to remove events with high curvature. This step removes about 12 dB of noise, but the overlap amplitude is still much bigger than the signal amplitude. During step 2 (Figure 4c) the overlap signal is estimated and removed: after removing the time gaps between adjacent shots to make the blended noise coherent and the signal incoherent in the common channel domain, a rank-reduction filter with rank 3 is applied. The value of 3 for the rank, chosen after the parametric analysis, was a compromise between removing enough noise (the higher the rank, the more blending noise is estimated and

subsequently removed) and preserving the signal. This step 2 determines an overall amplitude drop of 10 dB.

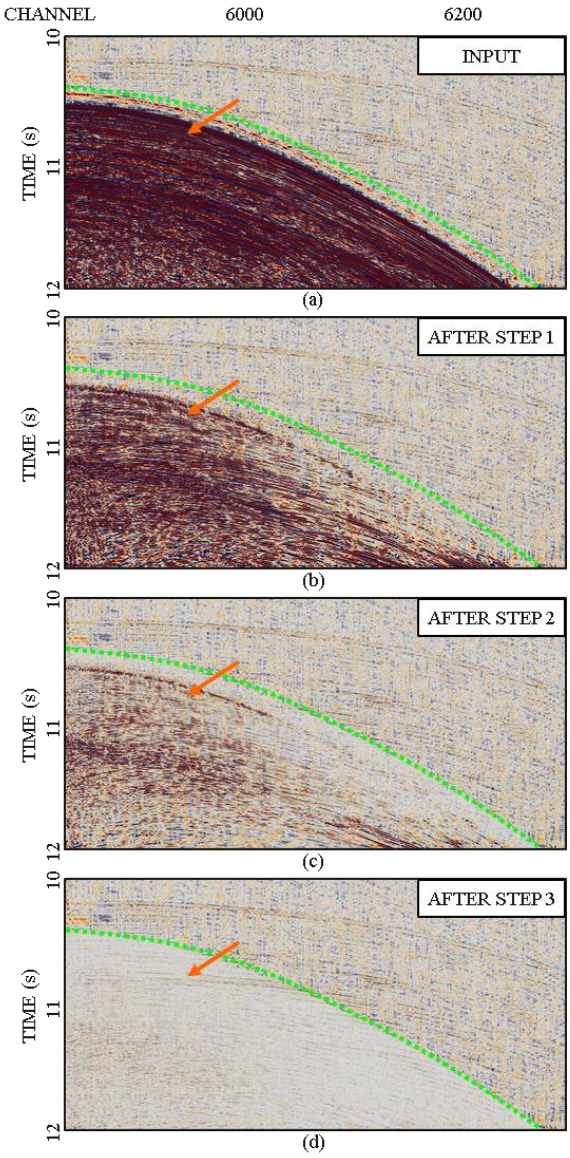

Figure 4: De-blending of a shot record: zoom (green rectangle in Figure 3a). The green dashed line is a reference for comparisons. The orange arrows indicates a coherent event retrieved by the de-blending process. a) input dataset; b) after step 1; c) after step 2; d) after step 3.

Finally during step 3 (Figure 4d) a rank 1 robust rank-reduction filter with is applied in the common channel gather after adding back the time gaps between adjacent shots. The choice of rank 1 was also determined by a parametric analysis on a synthetic dataset. A rank of 1 means that in each processing window the filter preserves only one dip and it would not be able to preserve crossing events. However, given the amount of blending noise in the overlap area, we aim for a result where the blending noise is almost completely attenuated, even if this means preserving only part of the signal. The amplitude level dropped by about 10 db after this final processing step. Overall, after step 3 the data amplitudes in the overlap area are about 5 dB lower that the amplitude outside the overlap area. This feature is expected due to the harshness of the filter, but it is still an acceptable compromise, because it allows the recovery of signal that would otherwise have been lost.

No strong reflectors are apparent below 10s, however we can note that the de-blending process is able to retrieve some coherent energy, indicated by the orange arrow in Figure 4a-d. This event is the second order water-bottom multiple of the primary that appears around 4s in Figure 3. The correct retrieval of multiples will improve the performance of SRME, that would otherwise create artifacts at this location. This event is clearly visible above the green dashed line, and continues below it, even if with attenuated amplitude. The retrieval of this multiple demonstrates that the de-blending methodology performs as expected, and it would also be able to identify primaries whenever present.

Figure 5 shows the stack of the line. Figure 5a illustrates the dataset before de-blending, Figure 5b the dataset after de-blending, Figure 5c the stack of the first 8s of the data, i.e. the standard acquisition without signal overlaps. Comparing Figure 5a-b with Figure 5c we can note that the record length extension from 8 to 12 s allows the Permian marker to be visualized (blue arrows in Figure 5a-b). However we must note that only the direct arrival (orange arrows in Figure 5a-b) is present in the first 10s of data, and therefore step 1 of the algorithm would be sufficient to de-blend the dataset up to the Permian 2-way time.

The data improvements generated by the application of step 2 and 3 are more difficult to evaluate, because strong reflectors are not present below the Permian marker. Figure 6 a shows a zoom of the stack (green rectangle in Figure 5a). Figure 6a shows the blended dataset, Figure 6b the de-blended, and Figure 6c the result that we would have obtained muting out the overlap area instead of de-blending it. The differences between Figure 6b and Figure 6c are subtle. This is expected, because a surgical mute would still preserve the long offsets recording of each event: in other words, the de-blending process increases the fold below 10s, adding near offset traces. However, we can note an

improvement in Figure 6b compared to Figure 6c: the random noise in the area is lower and some events (see the green arrows) are easier to identify after de-blending.

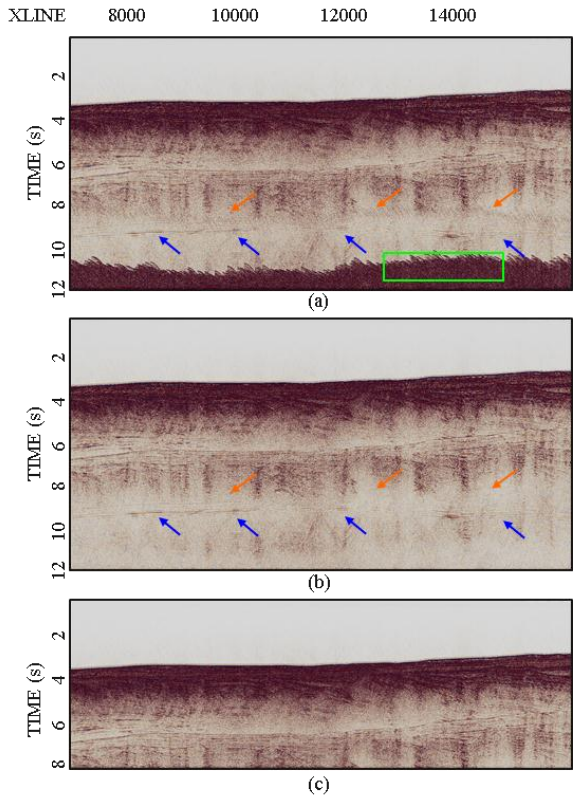

Figure 5: Stack. The blue arrows indicate the Permian marker, the orange arrows indicates the position of the direct arrival interference. The green rectangle indentificates the area zoomed in Figure 6. a) before de-blending; b) after de-blending; c) signal up to 8 s, i.e. standard acquisition, without signal overlap.

From these examples we can draw some considerations on the record length extension technique:

- The area above the blended water bottom primary can be cleaned almost perfectly, because it is straightforward to remove the direct arrival. A continuous recording acquisition can then be designed taking into account that the dataset will be unaffected by blending noise (after removing the direct arrival) for a lapse of time that is the time gap between adjacent sources plus the water bottom primary two-way travel time. This is relevant for deep water acquisition like Carnarvon.
- The area below the blended water bottom primary can not be cleaned perfectly, however the de-blending improves the signal to noise ratio of the stack. Since this blended data is always recorded, it requires no additional acquisition costs.

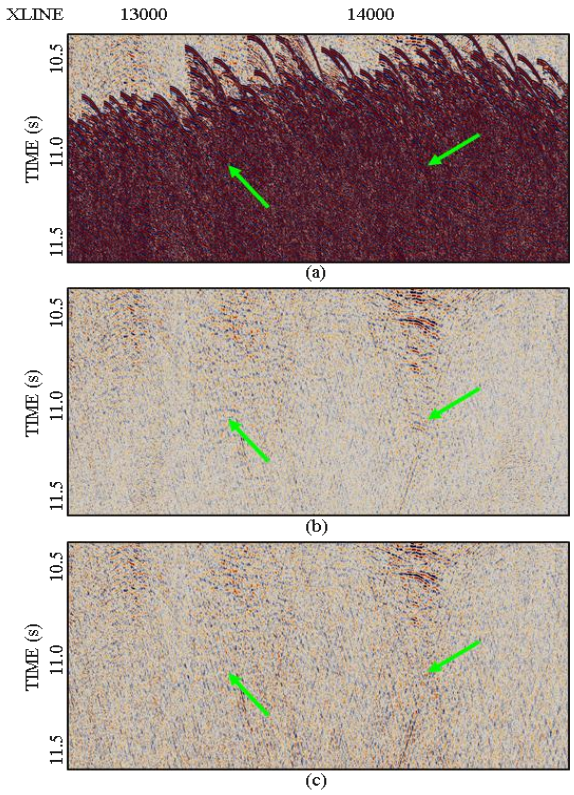

Figure 6: Stack: zoom (green rectangle in Figure 5a). The green arrows indicate events that are retrieved by the de-blending, and would have been lost muting the overlap. (a before de-blending; b) after de-blending; c) after surgical mute of the overlap.

Conclusions

This abstract describes the advantages of record length extension in the processing of the Carnarvon dataset. This dataset is acquired with continuous recording, with a shot-point time interval of 8s, and a processing trace length of 12s.The record length extension, together with the de-blending algorithm, allows the identification of the Permian marker, one of the targets of the survey, which is positioned at about 9.5s. The de-blending algorithm is composed of 3 steps. The first one, that includes *f-k* and Radon filters, allows the direct arrival to be removed from the dataset, de-blending it up to about 10.5s. The other 2 steps, based on rank-reduction filters in the common channel domain, improve the signal to noise ratio of the dataset below 10.5s.

Acknowledgements

The North Carnarvon 3D Data is courtesy of Dolphin Geophysical and TGS. We thank Dolphin's management for the permission to publish these results.

Rank-reduction de-blending for record length extension

Berkhout, A.J., 2008, Changing the mindset in seismic data acquisition: The Leading Edge, **27**, 924.

Cheng, J. and M.D. Sacchi, 2015, Separation and reconstruction of simultaneous source data via iterative rank-reduction: Geophysics, **80** (4), V57-V66.

Kumar, R., H. Wason, F.J. Herrmann, 2015, Source separation for simultaneous towed-streamer marine acquisition - A compressed sensing approach: Geophysics **80** (6), WD73-WD88.

Mahdad, A., P. Doulgeris, and G. Blacquiere, 2011, Separation of blended data by iterative estimation and subtraction of blending interference noise: Geophysics **76** (3), Q9-Q17.

Maraschini, M., R. Dyer, K. Stevens, and D. Bird, 2012, Source separation by iterative rank-reduction - Theory and applications: 74th EAGE, Extended Abstracts, A044.

Maraschini, M., A. Kielius, J. Barnes, S. Grion, 2016, Record-length extension by rank-reduction de-blending: 78th EAGE, Extended Abstracts.

Trickett, S.R., 2003, F-xy eigenimage noise suppression. Geophysics, 68 (2), 751-759.

Trickett, S.R., L., Burroughs, and A. Milton, 2012, Robust rank-reduction filtering for erratic noise. SEG Technical Program Expanded Abstracts 2012:1-5.

Wason, H., R. Kumar, F.J. Herrmann, and A.Y.Aravkin, 2014, Source separation via SVD-free rank minimization in the hierarchical semi-separable representation. SEG Technical Program Expanded Abstracts 2014: 120-126.